Click Here for Full Article

Estimate of the impact of absorbing aerosol over cloud on the MODIS retrievals of cloud optical thickness and effective radius using two independent retrievals of liquid water path

Eric M. Wilcox,[1] Harshvardhan,[2] and Steven Platnick[1]

[1] Two independent satellite retrievals of cloud liquid water path (*LWP*) from the NASA Aqua satellite are used to diagnose the impact of absorbing biomass burning aerosol overlaying boundary-layer marine water clouds on the Moderate Resolution Imaging Spectrometer (MODIS) retrievals of cloud optical thickness (τ) and cloud droplet effective radius (r_e). In the MODIS retrieval over oceans, cloud reflectance in the 0.86-μm and 2.13-μm bands is used to simultaneously retrieve τ and r_e. A low bias in the MODIS τ retrieval may result from reductions in the 0.86-μm reflectance, which is only very weakly absorbed by clouds, owing to absorption by aerosols in cases where biomass burning aerosols occur above water clouds. MODIS *LWP*, derived from the product of the retrieved τ and r_e, is compared with *LWP* ocean retrievals from the Advanced Microwave Scanning Radiometer-EOS (AMSR-E), determined from cloud microwave emission that is transparent to aerosols. For the coastal Atlantic southern African region investigated in this study, a systematic difference between AMSR-E and MODIS *LWP* retrievals is found for stratocumulus clouds over three biomass burning months in 2005 and 2006 that is consistent with above-cloud absorbing aerosols. Biomass burning aerosol is detected using the ultraviolet aerosol index from the Ozone Monitoring Instrument (OMI) on the Aura satellite. The *LWP* difference (AMSR-E minus MODIS) increases both with increasing τ and increasing OMI aerosol index. During the biomass burning season the mean *LWP* difference is 14 g m^{-2}, which is within the 15–20 g m^{-2} range of estimated uncertainties in instantaneous *LWP* retrievals. For samples with only low amounts of overlaying smoke (OMI $AI \leq 1$) the difference is 9.4, suggesting that the impact of smoke aerosols on the mean MODIS *LWP* is 5.6 g m^{-2}. Only for scenes with OMI aerosol index greater than 2 does the average *LWP* difference and the estimated bias in MODIS cloud optical thickness attributable to the impact of overlaying biomass burning aerosol exceed the instantaneous uncertainty in the retrievals.

1. Introduction

[2] Satellite measurements of visible and near-infrared reflectance are now used routinely to simultaneously retrieve cloud optical thickness (τ) and cloud drop effective radius (r_e). These data are used in climate studies, among other applications, to evaluate the radiative impact of clouds on the climate system [e.g., *Han et al.*, 1994; *Quaas et al.*, 2006]. These retrievals, however, may be biased in cases where a layer of absorbing aerosol resides above the cloud. This situation occurs frequently over the eastern South Atlantic Ocean during austral winter when smoke from extensive biomass burning in southern Africa is transported westward over a region of persistent low stratocumulus cloud cover. If the layer of absorbing biomass burning aerosol attenuates the sunlight that is both incident on and reflected by the top of the cloud, then the radiance measured by the satellite will imply a weaker cloud reflectance than that of the true cloud. This bias in estimated reflectance can result in a low bias retrieval for cloud optical thickness, and for retrievals based on certain wavelength band combinations, a biased retrieval in effective radius as well.

[3] *Haywood et al.* [2004] computed the expected bias in the cloud property retrieval on the basis of a radiative transfer model and in-situ measurements of aerosol optical properties. They report a low bias of up to 30% in τ for retrievals that depend on 0.63- or 0.86-μm reflectance values. Biases in r_e were found to be less than 1 μm for

[1]Climate and Radiation Branch, Laboratory for Atmospheres, NASA Goddard Space Flight Center, Greenbelt, Maryland, USA.
[2]Department of Earth and Atmospheric Sciences, Purdue University, West Lafayette, Indiana, USA.
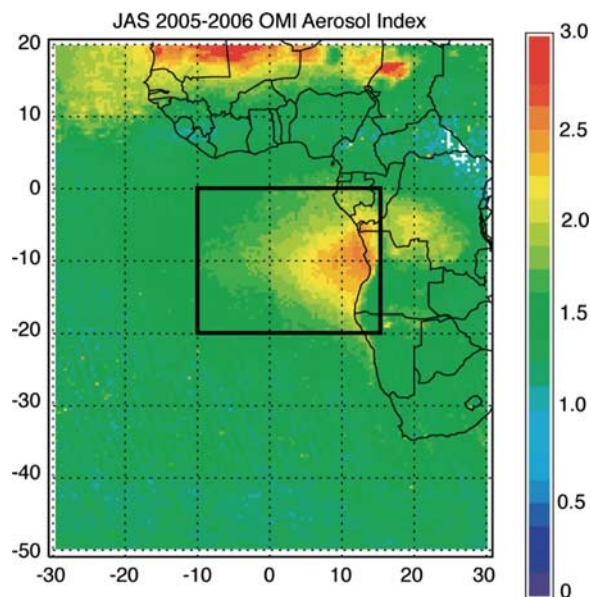
Figure 1. July, August, and September 2005–2006 average OMI aerosol index. The box indicates the geographic bounds applied to the data in this analysis.

retrievals where the visible reflectance is paired with the 3.7- or 2.13-μm reflectance. However, use of the 1.63-μm reflectance for the retrieval of r_e can result in underestimates of r_e of several μm. Biases in the retrieval of τ were greatest for bright clouds with high values of τ. *Haywood et al.* [2004] and *Cattani et al.* [2006] both presented case studies from several Moderate Resolution Imaging Spectrometer (MODIS) granules indicating a bias in the 1.63-μm r_e retrieval relative to the 2.13-μm retrieval.

[4] *Bennartz* [2007] found that the cloud liquid water path (*LWP*) retrieved from the Advanced Microwave Scanning Radiometer-EOS (AMSR-E) is systematically larger than the MODIS *LWP* derived from the τ and r_e retrievals for observations offshore of southern Africa during the biomass burning season; both sensors are on the NASA Aqua satellite. *Bennartz and Harshvardhan* [2007] argued that the difference between the AMSR-E and MODIS is qualitatively consistent with the reduced cloud optical thickness owing to absorbing aerosol overlying the cloud as estimated by *Haywood et al.* [2004]. Here we seek to confirm this explanation by relating the difference between AMSR-E and MODIS *LWP* directly to observations of absorbing aerosol over low clouds for a study region off the coast of Angola/Namibia.

[5] Furthermore, model simulations reported by *Johnson et al.* [2004] indicate that the heating above the boundary layer attributable to solar absorption by biomass burning aerosols overlaying stratocumulus clouds can enhance the strength of the inversion capping the boundary layer, thereby inhibiting cloud-top entrainment and allowing the cloud *LWP* to increase. Unraveling the impacts of aerosols on clouds using satellite data in this region requires an understanding of the impact of smoke on cloud property retrievals.

[6] In this study we diagnose the magnitude of the *LWP* bias in the Aqua MODIS cloud property retrieval using the

simultaneous and independent microwave *LWP* retrieval from AMSR-E. The microwave emission signal from clouds is not impacted by the presence of aerosol. The magnitude of the bias is reported as a function of increasing ultraviolet aerosol index determined from the nearly simultaneous Ozone Monitoring Instrument (OMI) observation on the NASA Aura satellite. Below a certain level of aerosol index, it is found that the bias in the MODIS *LWP* is less than the estimated uncertainties and the spatial/temporal RMS variability in the retrievals.

2. Methodology

[7] This study makes use of two independent remote sensing retrievals of *LWP* from the NASA Aqua satellite: MODIS solar reflectance retrievals that may be susceptible to biases in cases of absorbing aerosol overlying cloud, and the AMSR-E passive microwave retrievals using wavelengths that are transparent to aerosols. We seek to estimate the impact of above-cloud absorbing biomass burning aerosol on the MODIS retrieval by investigating any systematic relative bias between the two *LWP* retrievals with increasing absorbing aerosol amount above cloud. The aerosol is detected using the OMI aerosol index (*AI*), which is observed from the Aura satellite following the Aqua satellite approximately 15 minutes behind in the same orbit.

[8] *LWP* and *AI* observations are obtained for the oceanic region offshore of southern Africa bounded by 10 W to 15 E longitude and 20 S to 0 S latitude during July, August, and September 2005 and 2006. Aerosols emanating from the burning of the African Savannah are clearly evident over this region of ocean in satellite imagery (Figure 1). The OMI *AI* detects the presence of aerosols that absorb UV radiation, including in cases where the aerosols are present over stratocumulus clouds. The mean single scatter albedo of biomass burning aerosols observed during the Southern African Regional Science Initiative (SAFARI) 2000 field campaign was 0.91 ± 0.04 at 0.55 μm and 0.86 at 0.87 μm based on in-situ measurements from the study of *Haywood et al.* [2004].

[9] The vertical profiles of the biomass burning aerosol layers were also observed over the South Atlantic Ocean during SAFARI 2000. These aerosols were typically observed in layers that were vertically separated from stratocumulus clouds below [*Hobbs*, 2002; *McGill et al.*, 2003; *Haywood et al.*, 2003]. These observations imply that direct microphysical interaction between the aerosols and stratocumulus clouds is often inhibited by the strong temperature inversion above the cloud layer.

[10] MODIS *LWP* is derived from the τ and r_e retrievals in the operational Aqua MODIS Level-2 collection 5 MYD06 product. These parameters are retrieved for pixels determined to be overcast and assumed to be homogeneous [*Platnick et al.*, 2003]. A nonabsorbing visible or near-infrared spectral band provides the principle sensitivity to τ. The 0.86-μm reflectance is used for the ocean retrievals evaluated in this study. The absorbing near-infrared reflectance at 2.13 μm provides the principle sensitivity to r_e. In situ observations of marine stratocumulus clouds in the study area indicate that their vertical structure is adiabatic with the cloud drop radius increasing with height through the cloud [*Keil and Haywood*, 2003]. *LWP* for adiabatic clouds is

Table 1. LWP_{AMSR-E}, LWP Difference (LWP_{AMSR-E} minus LWP_{MODIS}), τ Uncertainty, and LWP_{MODIS} Uncertainty Statistics for All Overcast Samples and Overcast Samples of Various OMI AI Ranges[a]

	All AI	$AI \leq 1$	$1 < AI \leq 2$	$2 < AI \leq 3$	$AI > 3$
Number of samples	43,140	21,206	17,012	4354	568
Mean LWP_{AMSR-E}	92	90	92	95	103
Median LWP_{AMSR-E}	80	80	80	80	100
Estimated τ uncertainty	1.4	1.4	1.4	1.4	1.2
Estimated LWP_{MODIS} uncertainty	19 (1.4)	20 (1.5)	18 (1.4)	17 (1.3)	16 (1.2)
Mean LWP difference (RMS)	14 (18)	9.4 (15)	16 (19)	23 (23)	34 (25)

[a]LWP_{MODIS} uncertainty assumes that all pixel-level uncertainties are correlated. LWP_{MODIS} uncertainty values in parentheses assume that only daily uncertainties are correlated while uncertainties from different days are uncorrelated. RMS values of LWP difference are enclosed in parentheses. All units are in g m^{-2} except for the number of samples and τ uncertainty.

derived from the product of r_e and τ ($LWP \approx 5/9 r_e \tau$ [see *Wood and Hartmann*, 2006]).

[11] The AMSR-E retrieval of LWP for low clouds over ocean relies on the emission signal of condensed water using the algorithm of *Wentz* [1997] and *Wentz and Spencer* [1998]. The algorithm retrieves LWP as part of a unified scheme for retrieving surface wind speed, column water vapor, LWP, and rain rate simultaneously using 5 channels of AMSR-E ranging from 6.9 GHz to 89 GHz. The retrieval is only performed over ocean because of the challenge of constraining the surface emission over land where the surface emissivity is highly variable. We use the daily 0.25° gridded products provided by Remote Sensing Systems (available from www.remss.com/amsr/amsr_browse.html).

[12] The AMSR-E gridded LWP is an average over the entire 0.25° area, while the MODIS LWP is reported only for pixels (~1 km at nadir) determined to be overcast. Therefore the values are only comparable for 0.25° grid cells that are confidently determined as overcast. We average the pixels reporting a valid MODIS LWP for each 0.25° grid cell, however only grid cells with 100% of MODIS pixels reporting a valid LWP are included in our analysis. Because of the screening applied to the pixel-level τ and r_e retrievals, this represents a conservative screening for overcast conditions. Furthermore, only grid cells with average MODIS cloud-top temperature greater than 273 K and zero AMSR-E rain rate are included.

[13] The presence of absorbing aerosol layers above cloud is observed with the OMI sensor on the Aura satellite. The OMI aerosol index is derived from the ratio between the upwelling intensity at 331 nm and the intensity at 360 nm. The index reflects the difference in the spectral contrast between these frequencies and the spectral contrast derived from a radiative transfer model of a purely Rayleigh scattering atmosphere and a Lambertian surface [*Herman et al.*, 1997; *Torres et al.*, 1998]. The aerosol index as applied to OMI is given as [*Ahmad et al.*, 2006]

$$\text{OMI } AI = -100 \left[\log_{10}\left(\frac{I_{331}}{I_{360}} \right)_{meas} - \log_{10}\left(\frac{I_{331}}{I_{360}} \right)_{calc} \right]$$

where I_λ is the intensity at the specified wavelength and the subscripts "meas" and "calc" indicate the measured and model calculated quantities respectively. In a clear Rayleigh scattering atmosphere with low surface reflectivity (such as the ocean or land in the UV wavelengths considered here), the reflectivity of UV radiation in the 330 to 380 nm range decreases with increasing wavelength. Absorbing aerosols such as biomass burning emissions reduce the reflectivity

by absorbing radiation and by reducing molecular scattering in and below the aerosol layer. Furthermore, UV-absorbing aerosols reduce the spectral contrast, even leading to cases where reflectance increases with wavelength [*Hsu et al.*, 1996]. Thus absorbing aerosols lead to positive values of the OMI AI. AI increases approximately linearly with the UV optical depth with a slope that increases with decreasing single scatter albedo [*Torres et al.*, 1998]. Clouds enhance UV reflectivity with only a weak spectral signature, and therefore do not interfere with the detection of overlying absorbing aerosol.

[14] OMI data are obtained from the level 2 gridded products, which provide OMI AI footprints (13 × 24-km size at nadir) arranged on the 0.25° grid. Where more than one OMI AI footprint is centered within a single grid cell, the AI values are averaged. Because of the relatively large OMI footprint, some grid cells at the edge of the OMI swath do not encompass the center point of a singe OMI footprint. These grid cells are ignored in the following analysis.

[15] Averages of the instantaneous difference between the two LWP retrievals are evaluated against the magnitude of the estimated uncertainties in the two retrievals. *Wentz* [1997] estimates the uncertainty in instantaneous microwave LWP retrievals (based on special sensor microwave/imager data) to be 25 g m^{-2}. More recent examinations of cloud-cleared microwave imager data indicate average systematic uncertainties in instantaneous LWP retrievals from 7 g m^{-2} (based on AMSR-E [*Greenwald et al.*, 2007]) to 15 g m^{-2} (based on TRMM Microwave Imager data [*Horváth and Gentemann*, 2007]). Average estimated random error in the AMSR-E data is 13 g m^{-2} [*Greenwald et al.*, 2007]. Estimated uncertainties for τ and LWP_{MODIS} are reported in Table 1. These are provided for each pixel in the MYD06 products, and are intended as minimum uncertainties that account for estimated calibration and model uncertainty, estimated uncertainty in the surface albedo, and estimated uncertainty in the above-cloud precipitable water amount. Other error sources may be present, such as horizontal inhomogeneity, which are not accounted for. The average estimated instantaneous uncertainty in τ is 1.4 (11% of mean τ), but increases for higher values of τ (see discussion of Figure 3 below). The average estimated instantaneous uncertainty in LWP_{MODIS} is 19 g m^{-2}. Allowing for the possibility that only daily uncertainties are correlated reduces the estimated LWP_{MODIS} uncertainty to 1.4 g m^{-2} for averages of 180 days of data. Adopting the AMSR-E values noted above from the work of *Greenwald et al.* [2007] yields a combined uncertainty for instantaneous observations of the LWP difference of ±24 g m^{-2}. RMS
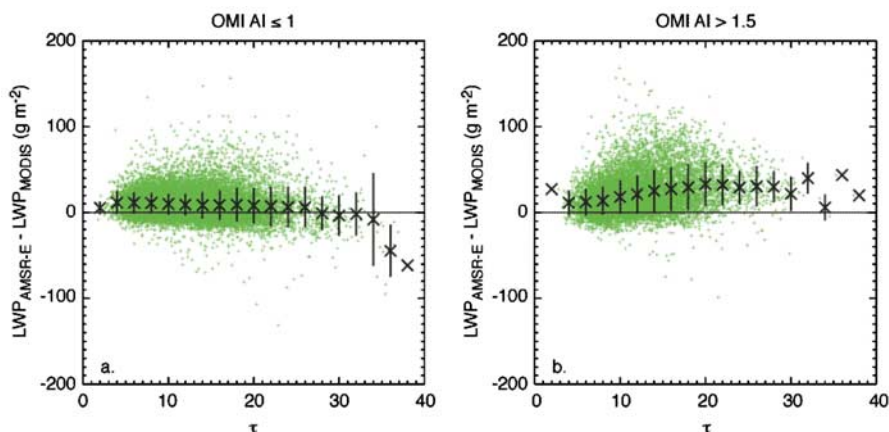
Figure 2. *LWP* difference (AMSR-E minus MODIS) against MODIS cloud optical thickness for all overcast samples. Green pluses are individual 0.25° gridded samples. Crosses are averages for τ bins of 2-unit width. Vertical lines indicate standard deviations of τ bin averages. For each pair, the samples on the left correspond to OMI $AI \leq 1.0$ and on the right to OMI $AI > 1.5$.

variability of the *LWP* difference for all samples included in this study is 18 g m^{-2} (Table 1).

3. Results

[16] Figure 2 shows the *LWP* difference (AMSR-E minus MODIS) as a function of τ for July, August and September 2005 and 2006. Shown on the left are cases with OMI *AI* less than or equal to 1, and on the right are cases with OMI *AI* greater than 1.5. Averages and standard deviations are shown for τ bins of 2-unit width. For cases of OMI $AI \leq 1$, indicating no smoke, or only small amounts of smoke overlaying the cloud, LWP_{MODIS} and LWP_{AMSR-E} agree on average to within ±10 g m^{-2} in most τ bins, with standard deviations representing temporal/spatial variability of approximately ±20 g m^{-2}. The average *LWP* difference for these low smoke cases is 9.4 g m^{-2}. Note that these cases include a relatively small number of samples with OMI $AI <$ 0, which generally indicate the presence of a scattering aerosol.

[17] For cases with OMI $AI > 1.5$, indicating the presence of absorbing aerosol over the clouds, the *LWP* difference is greater than that for the $AI \leq 1$ cases and increases with increasing τ. *Haywood et al.* [2004] demonstrated with a radiative transfer model that for the 0.86/2.13-μm MODIS cloud retrieval over oceans, absorption by biomass burning aerosols reduces the 0.86-μm retrieval of τ compared to the retrieval from nonpolluted scenes. Furthermore, they found that the low bias in τ attributable to the influence of absorbing aerosol increases with increasing 0.86-μm reflectance; that is, the bias increases with τ. A low bias in τ would lead to a proportional low bias in LWP_{MODIS}. The results shown in Figure 2 are consistent with the *Haywood et al.* [2004] result.

[18] An estimate of the LWP_{MODIS} bias attributable to the smoke aerosols indicated in Figure 2 is made by subtracting the average *LWP* difference from each τ bin under low OMI *AI* conditions in Figure 2a from each *LWP* difference sample with OMI $AI > 1.5$. The τ bias necessary to yield the *LWP* difference attributable to the smoke is computed using the relationship between *LWP*, τ and r_e described in

section 2 above and displayed in Figure 3. This quantity decreases with increasing τ to about −4 for clouds of τ equal to 20 to 25. The instantaneous uncertainty in the τ retrievals for these clouds is of about the same magnitude (red dashed lines), as is the RMS variability of the estimated τ bias (black error bars).

[19] Figure 4 shows the differences between averages of high OMI *AI* samples and low OMI *AI* samples in each τ bin for LWP_{AMSR-E} (top), LWP_{MODIS} (middle) and r_e (bottom). *LWP* and τ are positively correlated. Because τ is underestimated in the high OMI *AI* samples owing to the effect of the smoke aerosols, these samples have a higher
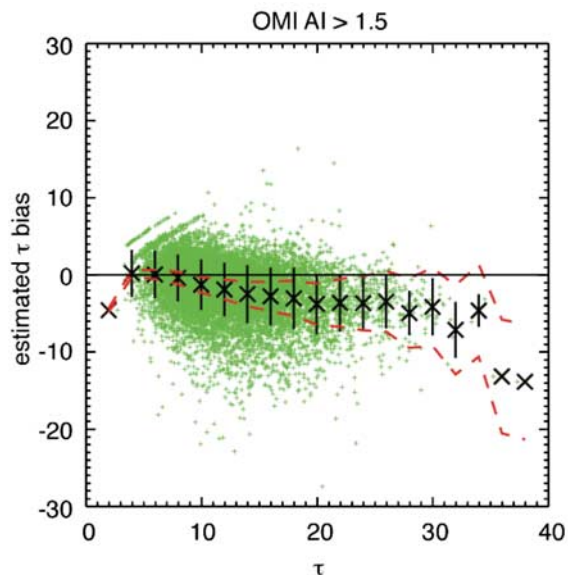

Figure 3. Estimated bias in MODIS cloud optical thickness for samples with OMI $AI > 1.5$ against τ for all overcast samples. Green pluses are individual 0.25° gridded samples. Crosses are averages for τ bins of 2-unit width. Vertical lines indicate standard deviations of τ bin averages. Red dashed lines indicate the range of estimated instantaneous uncertainty in the MODIS τ retrieval.
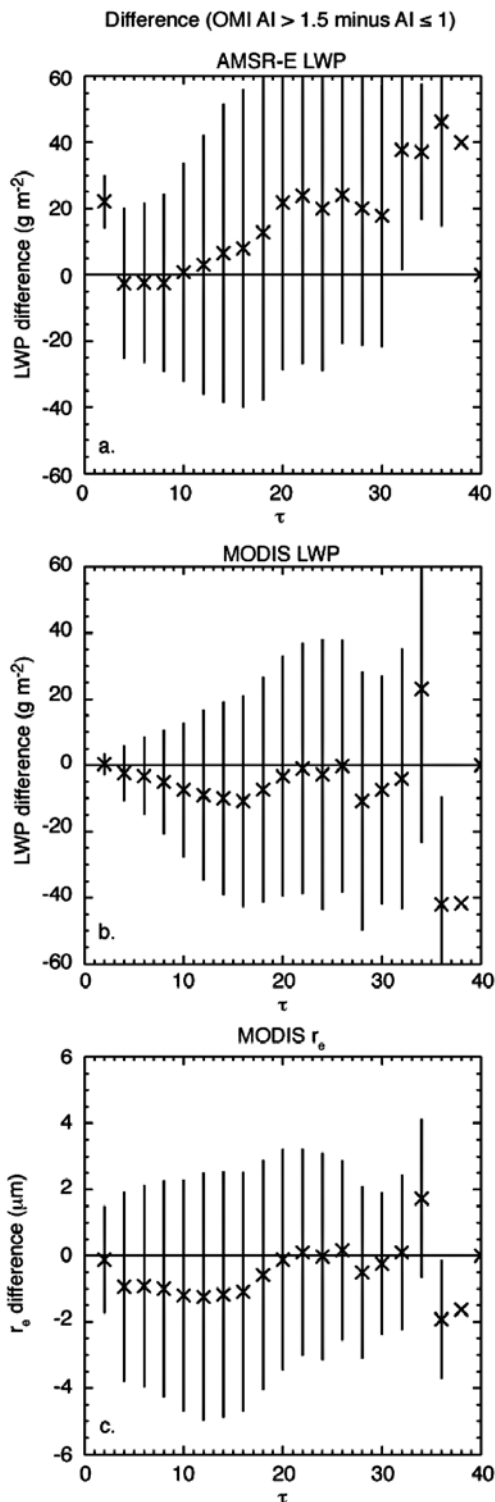
Figure 4. *LWP* and r_e differences between high OMI *AI* samples (*AI* > 1.5) and low OMI *AI* samples (*AI* ≤ 1) against MODIS cloud optical thickness. Crosses are differences of averages over τ bins of 2-unit width. Vertical lines are the sum (in quadrature) of the standard deviation of the clean cases and the polluted cases in each τ bin. (top) LWP_{AMSR-E}, (middle) LWP_{MODIS}, and (bottom) r_e (MODIS).

LWP_{AMSR-E} than low OMI *AI* samples. The effect of the absorbing aerosol on the τ retrieval becomes apparent for clouds with τ above about 10, and increases with τ as noted above. Only a few samples have $\tau > 30$, leading to poor sampling statistics for these τ bins. Differences of 10 g m^{-2} or less are found for averages of LWP_{MODIS} between high OMI *AI* and low OMI *AI* samples in most τ bins. No difference is expected as a consequence of the bias in τ because both the retrieved τ and the inferred LWP_{MODIS} in Figure 4 (middle) are similarly affected. However, a significant difference might be expected if a corresponding bias were present in the r_e retrieval for the smoke-affected samples. Figure 4 (bottom) confirms that differences in r_e between high and low OMI *AI* samples are 1 μm or less. *Haywood et al.* [2004] found that absorption by biomass burning aerosols introduced low biases in r_e of not more than 1 μm in simulated retrievals with the 0.86/2.13-μm bands used in the MODIS retrieval over oceans.

[20] For comparison, *LWP* differences (AMSR-E minus MODIS) are shown for OMI *AI* ≤ 1 cases over the Southeast Pacific Ocean (Figure 5). In the absence of biomass burning or other sources of absorbing aerosol, nearly every sample in this region from the 180-day period exhibits OMI *AI* values less than or equal to 1. In contrast to the Southeast Atlantic Ocean during the same season, there is a systematic *LWP* difference for overcast marine boundary-layer clouds that increasingly favors LWP_{MODIS} for increasing τ. The difference might be attributable to geographic differences in cloud structure. This study applies a retrieval of LWP_{MODIS} that assumes an adiabatic cloud structure ($LWP \approx 5/9r_e\tau$). The *LWP* retrieval in the standard MODIS product assumes a uniform vertical cloud structure ($LWP \approx 2/3r_e\tau$ [see *Stephens*, 1978]). When computing the *LWP* difference using the uniform cloud profile retrieval for the Southeast Atlantic clouds, a similar bias is found that increasingly favors MODIS for increasing τ (not shown). While changing the retrieval algorithm applied to MODIS removed this systematic difference for Southeast Atlantic Ocean cases (Figure 2), it did not for Southeast Pacific Ocean cases. Aircraft observations indicate that the effective radius of cloud drops generally increase through the depth of the cloud [*Keil and Haywood*, 2003]. This increase is linear in height above cloud base in the adiabatic cloud model. It is important to note that the retrieval applied here assumes the retrieved r_e is at the very top of the cloud. Weighting functions for MODIS retrievals of r_e and τ are reported by *Platnick* [2000] where it is found that the retrievals include reflectance contributions from a layer at the top of the cloud. As a result, biases in retrieved *LWP* assuming uniform vertical cloud structure are only 3% to 10% for modeled adiabatic clouds; smaller than expected. Additionally, entrainment drying at cloud top can reduce cloud drop sizes near cloud top below the size expected from the adiabatic model.

[21] The mean difference between LWP_{AMSR-E} and LWP_{MODIS} is reported in Table 1 for all overcast samples and for overcast samples within various ranges of OMI *AI*. The average *LWP* difference (AMSR-E minus MODIS) is 14 g m^{-2}. For samples with only low amounts of overlaying smoke (OMI *AI* ≤ 1), however, the difference is 9.4 g m^{-2}. This difference of 5.6 g m^{-2}, attributable to the impact of aerosols on the MODIS retrieval, is less than the uncertainty
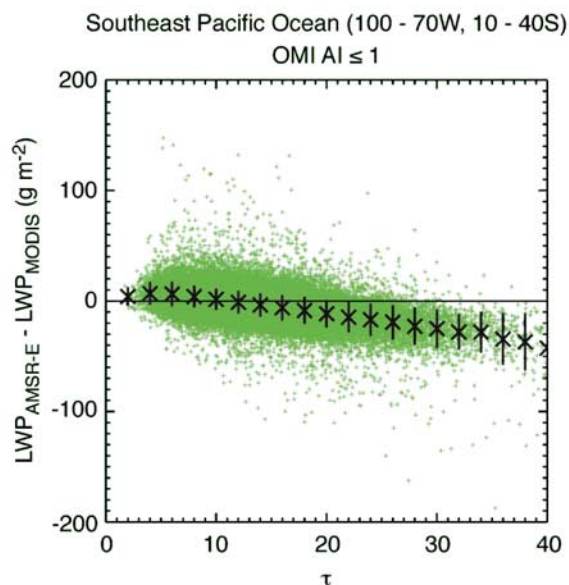
Figure 5. July, August, and September 2005–2006 *LWP* difference (AMSR-E minus MODIS) against τ for all overcast samples in the South Pacific stratocumulus region with OMI $AI \le 1$ (only a few samples exhibited OMI AI values > 1). Green pluses are individual 0.25° gridded samples. Crosses are averages over τ bins of 2-unit width. Vertical lines indicate standard deviations of τ bin averages.

in instantaneous *LWP* retrievals from either instrument (15 g m^{-2} and 19 g m^{-2} for AMSR-E and MODIS respectively) or the RMS variability of the *LWP* difference (18 g m^{-2}). *Bennartz* [2007] reported differences in area averaged *LWP* during the biomass burning season that favor LWP_{AMSR-E} by about 10 g m^{-2}. *Bennartz and Harshvardhan* [2007] attributed this difference to the smoke effect on the MODIS retrieval of τ. The results reported here indicate that part of this difference is independent of the smoke effect.

[22] The *LWP* difference between the highest OMI AI samples ($AI > 3$) and the lowest OMI AI samples ($AI \le 1$) is 24.6 g m^{-2} and indicates the maximum impact of smoke aerosol on LWP_{MODIS}. The *LWP* difference increases sys-

tematically with increasing OMI AI. This dependence is shown in Figure 6 (left) and suggests a low bias in the MODIS retrieval of τ with a magnitude that increases with the aerosol amount. The *LWP* difference attributable to the impact of the aerosols is estimated by subtracting the mean *LWP* difference for all samples with OMI $AI \le 1$ from each instantaneous sample of the *LWP* difference. The estimated τ bias implied by this *LWP* difference attributable to the aerosol impact is computed using the relationship between *LWP*, τ and r_e described in section 2 and shown in Figure 6b. Only for those samples with OMI AI greater than 2 does this estimated bias in τ exceed the ±1.4 mean instantaneous uncertainty in the τ retrieval. These samples represent less than 9% of all overcast samples. The mean *LWP* difference for samples with $AI = 2$ is 20.5 g m^{-2}, which is comparable in magnitude to both the estimated instantaneous uncertainty in the MODIS retrieval and the RMS variability of the *LWP* difference. Only in a relatively small number of cases does biomass burning aerosol from Africa result in an impact on the τ and *LWP* retrievals of 20% or greater for stratocumulus clouds over the South Atlantic Ocean.

[23] Although the bias in MODIS τ and *LWP* retrievals owing to biomass burning aerosols only exceeds the other errors in these retrievals in a relatively few cases, the bias is detectable and present in regionally and seasonally averaged analyses [*Bennartz*, 2007; *Bennartz and Harshvardhan*, 2007]. This study indicates that with collocated observations in ultraviolet bands, such as provided by OMI, the samples subjected to such a bias can be identified and avoided. Alternatively, if microwave *LWP* observations are also available, it is possible to retain those samples and estimate the magnitude of the bias.

4. Summary

[24] Collocated MODIS, AMSR-E, and OMI data are used to identify cases of biomass burning aerosol overlaying boundary-layer stratocumulus clouds offshore of Western Africa during the July-September biomass burning seasons of 2005 and 2006. MODIS retrievals of τ and r_e are expected to be biased in cases where absorbing aerosol above a cloud layer is sufficient to reduce the visible/near-infrared cloud reflectance at the satellite sensor. The exis-
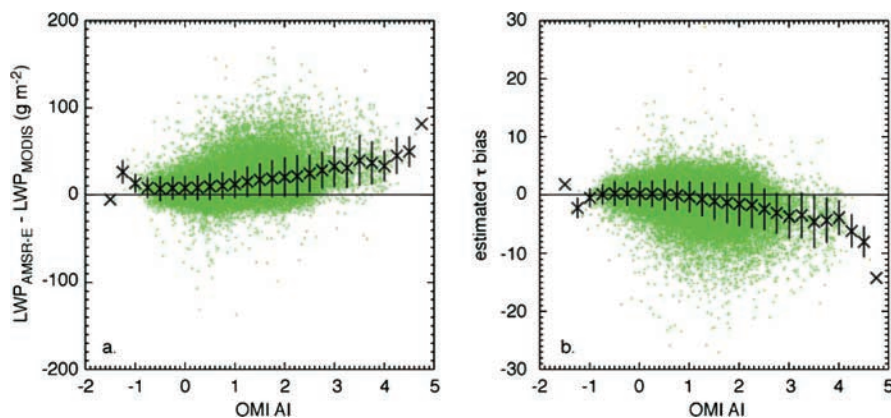

Figure 6. (left) *LWP* difference (AMSR-E minus MODIS) and (right) estimated τ bias against OMI AI for all overcast samples. Green pluses are individual 0.25° gridded samples. Crosses are averages for OMI AI bins of 0.25-magnitude width. Vertical lines indicate standard deviations of OMI AI bin averages.

tence and magnitude of this bias can be estimated using simultaneous retrievals of LWP from AMSR-E, which observes the microwave emissions from clouds that are transparent to aerosols. LWP_{MODIS} derived from the product of the retrieved τ and r_e is found to agree on average with LWP_{AMSR-E} to within ± 10 g m^{-2} for averages over τ bins across most of the range of observed τ. For Southeast Pacific Ocean cases with OMI ≤ 1, there is a systematic difference between LWP_{MODIS} and LWP_{AMSR-E} for overcast samples that increasingly favors LWP_{MODIS} for increasing τ which is not associated with the presence of biomass burning aerosol. For cases with a greater amount of smoke aerosols (OMI $AI > 1.5$), LWP_{MODIS} is biased low relative to LWP_{AMSR-E}, which is consistent with the expectation that the 0.86-μm MODIS radiances are reduced by the absorption in the aerosol layer, leading to a low bias in the τ retrieval. The r_e retrieval is only minimally impacted by the aerosol. The effect of absorbing biomass burning aerosols on the LWP_{MODIS} retrieval is 5.6 g m^{-2} on average, which is within the estimated instantaneous uncertainty for the LWP retrievals and within the RMS variability of individual samples of the LWP difference. The magnitude of the τ bias increases with τ and also increases with the magnitude of the OMI AI. Only for cases with OMI $AI > 2$, which account for about 9% of overcast samples, does the bias in LWP_{MODIS} relative to LWP_{AMSR-E} and the estimated bias in τ attributable to the impact of biomass burning aerosols exceed the instantaneous uncertainty of the retrievals.

References

Ahmad, S. P., O. Torres, P. K. Bhartia, G. Leptoukh, and S. Kempler (2006), Aerosol index from TOMS and OMI measurements, paper presented at 14th AMS Conference on the Applications of Air Pollution Meteorology with the Air and Waste Management Association, Am. Meteorol. Soc., Atlanta, Ga.

Bennartz, R. (2007), Global assessment of marine boundary layer cloud droplet number concentration from satellite, *J. Geophys. Res.*, *112*, D02201, doi:10.1029/2006JD007547.

Bennartz, R., and Harshvardhan (2007), Correction to "Global assessment of marine boundary layer cloud droplet number concentration from satellite", *J. Geophys. Res.*, *112*, D16302, doi:10.1029/2007JD008841.

Cattani, E., M. J. Costa, F. Torricella, V. Levizzani, and A. M. Silva (2006), Influence of aerosol particles from biomass burning on cloud microphysical properties and radiative forcing, *Atmos. Res.*, *82*, 310–327.

Greenwald, T. J., T. S. L'Ecuyer, and S. A. Christopher (2007), Evaluating specific error characteristics of microwave-derived cloud liquid water products, *Geophys. Res. Lett.*, *34*, L22807, doi:10.1029/2007GL031180.

Han, Q., W. B. Rossow, and A. A. Lacis (1994), Near-global survey of effective droplet radii in liquid water clouds using ISCCP data, *J. Clim.*, *7*, 465–497.

Haywood, J. M., S. R. Osborne, P. N. Francis, A. Keil, P. Formenti, M. O. Andreae, and P. H. Kaye (2003), The mean physical and optical properties of regional haze dominated by biomass burning aerosol measured from the C-130 aircraft during SAFARI 2000, *J. Geophys. Res.*, *108*(D13), 8473, doi:10.1029/2002JD002226.

Haywood, J. M., S. R. Osborne, and S. J. Abel (2004), The effect of overlying absorbing aerosol layers on remote sensing retrievals of cloud effective radius and cloud optical depth, *Q. J. R. Meteorol. Soc.*, *130*, 779–800.

Herman, J. R., P. K. Bhartia, O. Torres, C. Hsu, C. Seftor, and E. Celarier (1997), Global distribution of UV-absorbing aerosols from Nimbus 7/TOMS data, *J. Geophys. Res.*, *102*(D14), 16,911–16,922.

Hobbs, P. V. (2002), Clean air slots amid atmospheric pollution, *Nature*, *415*, 861.

Horváth, Á., and C. Gentemann (2007), Cloud fraction dependent bias in satellite liquid water path retrievals of shallow non-precipitating marine clouds, *Geophys. Res. Lett.*, *34*, L22806, doi:10.1029/2007GL030625.

Hsu, N. C., J. R. Herman, P. K. Bhartia, C. J. Seftor, O. Torres, A. M. Thompson, J. F. Gleason, T. F. Eck, and B. N. Holben (1996), Detection of biomass burning smoke from TOMS measurements, *Geophys. Res. Lett.*, *23*, 745–748.

Johnson, B. T., K. P. Shine, and P. M. Forster (2004), The semi-direct aerosol effect: Impact of absorbing aerosols on marine stratocumulus, *Q. J. R. Meteorol. Soc.*, *130*, 1407–1422.

Keil, A., and J. M. Haywood (2003), Solar radiative forcing by biomass burning aerosol particles during SAFARI 2000: A case study based on measured aerosol and cloud properties, *J. Geophys. Res.*, *108*(D13), 8467, doi:10.1029/2002JD002315.

McGill, M. J., D. L. Hlavka, W. D. Hart, E. J. Welton, and J. R. Campbell (2003), Airborne lidar measurements of aerosol optical properties during SAFARI-2000, *J. Geophys. Res.*, *108*(D13), 8493, doi:10.1029/2002JD002370.

Platnick, S. (2000), Vertical photon transport in cloud remote sensing problems, *J. Geophys. Res.*, *105*, 22,919–22,935.

Platnick, S., M. D. King, A. Ackerman, W. P. Menzel, B. A. Baum, J. C. Riédi, and R. A. Frey (2003), The MODIS cloud products: Algorithms and examples from Terra, *IEEE Trans. Geosci. Remote Sens.*, *41*, 459–473.

Quaas, J., O. Boucher, and U. Lohmann (2006), Constraining the total aerosol indirect effect in the LMDZ and ECHAM4 GCMs using MODIS satellite data, *Atmos. Chem. Phys.*, *6*, 947–955.

Stephens, G. L. (1978), Radiation profiles in extended water clouds. part II: Parameterization schemes, *J. Atmos. Sci.*, *35*, 2123–2132.

Torres, O., P. K. Bhartia, J. R. Herman, Z. Ahmad, and J. Gleason (1998), Derivation of aerosol properties from satellite measurements of backscattered ultraviolet radiation: Theoretical basis, *J. Geophys. Res.*, *103*, 17,099–17,110.

Wentz, F. J. (1997), A well-calibrated ocean algorithm for special sensor microwave/imager, *J. Geophys. Res.*, *102*, 8703–8718.

Wentz, F. J., and R. W. Spencer (1998), SSM/I rain retrievals within a unified all-weather ocean algorithm, *J. Atmos. Sci.*, *55*, 1613–1627.

Wood, R., and D. L. Hartmann (2006), Spatial variability of liquid water path in marine low cloud: The importance of mesoscale cellular convection, *J. Clim.*, *19*, 1748–1764.

————————

Harshvardhan, Department of Earth and Atmospheric Sciences, Purdue University, 550 Stadium Mall Drive, West Lafayette, IN 47907, USA.

S. Platnick and E. M. Wilcox, Climate and Radiation Branch, Laboratory for Atmospheres, NASA Goddard Space Flight Center, Code 613.2, Greenbelt, MD 20771, USA. (eric.m.wilcox@nasa.gov)